DRAFT VERSION 24TH JULY 2019
Preprint typeset using LaTeX style emulateapj v. 12/16/11

CORE MAGNETIC FIELD IMPRINT IN THE NONRADIAL OSCILLATIONS OF RED GIANT STARS

PEDRO GOMES[1]
[1]Centro de Astrofísica e Gravitação - CENTRA, Departamento de Física, Instituto Superior Técnico - IST, Universidade de Lisboa - UL, Av. Rovisco Pais 1, 1049-001 Lisboa

(Dated: 24th July 2019)
Draft version 24th July 2019

Abstract

A recent analysis performed to a group of red giants using asteroseismological data from the Kepler mission revealed that a considerable fraction of these stars exhibit dipole modes with very low visibilities. This phenomenon has been associated to the prevalence of strong magnetic fields ($\gtrsim 10^6$ G) in the cores of these stars, whose interaction with gravity waves prevents the formation of dipole modes with normal amplitudes. Using adequate stellar models and a novel semi-analytical method to solve the standard wave equation in the context of stellar oscillations, we studied the impact of wave transmission between the envelope and the core in the theoretical visibilities of depressed modes. Applying this method to the prescription discussed in the literature, we verified that our predictions reproduce the observed visibilities remarkably well. Since magnetic fields also influence the oscillations by introducing a frequency splitting, we calculated the necessary field strength to produce a 1 μHz splitting in the frequencies of oscillation modes of different angular degrees. Using two well established magnetic field configurations, validated by numerical simulations, we found that a field of 10^5 G in the core is necessary to produce this effect. This result has an impact on the strong field conjecture, as the strengths predicted by this hypothesis should lead to observable splittings. Moreover, considering the observational limits, we estimate that magnetic fields in the cores of red giants that do not show magnetic splittings cannot exceed 10^4 G.

1. INTRODUCTION

In the recent years, the sheer wealth and amount of data collected by the *CoRot* (Baglin et al. 2007) and Kepler space missions (Gilliland et al. 2010, Chaplin et al. 2011, Serenelli et al. 2017) has led to an enormous up-growth of knowledge regarding the structure and constitution of stars and allowed the testing of theories of stellar evolution and asteroseismology. This has certainly been the case in what concerns red giant stars, whose seismology allowed the precise measurement of core rotation rates (e.g., Beck et al. 2012) and the distinction between red giants undergoing hydrogen or helium burning (Bedding et al. 2011).

Following the cessation of nuclear reactions in the core due to hydrogen exhaustion, stars undergo core contraction simultaneously with envelope expansion. This duality leads to the coupling of acoustic, or pressure modes in the envelope to gravity modes in the core, forming a rich and complex mixed oscillation mode pattern that can be used to probe the star in all its extension (e.g., Chaplin and Miglio 2013). These oscillation modes arise from the interference of waves excited by near-surface turbulent convection, and, in other words, can be extremely useful in diagnosing the physical conditions in stellar interiors. The designation attributed to the acoustic modes stems from the fact that when the equilibrium state is disturbed, the restoring force is pressure, whereas in the case of gravity modes it is gravity through buoyancy (e.g. Aerts et al. 2010).

The mathematical treatment of stellar pulsation assumes that the oscillations occur adiabatically around an equilibrium state of spherical symmetry. As such, the oscillation modes are labelled by three quantum numbers, the radial order n, and the angular degree ℓ and azimuthal order m, which must satisfy $|m| \leqslant \ell$. The first is the number of nodes in the radial direction, between the centre of the star and the surface (e.g. Kippenhahn et al. 2012). In turn, the angular degree and azimuthal order concern the angular part and are the number of the nodes on the surface of the star and across the longitudinal direction, respectively. Because of the assumption of spherical symmetry, in the theory of linear adiabatic stellar pulsations, the eigenmodes of the system are degenerate and do not depend on m.

Magnetic fields in stars can be studied through the effect they have on stellar oscillations. For some time it has been known that weak magnetic fields lift the degeneracy and lead to the splitting of the frequencies of the oscillation modes (e.g., Ledoux & Simon 1957, Biront et al. 1982, Roberts & Soward 1983). This effect has been studied for the case of the Sun in what concerns acoustic and gravity modes (e.g., Gough and Taylor 1984, Gough and Thompson 1990, Rashba et al. 2007), AP stars (Dziembowski and Goode 1985), slowly pulsating B-stars (Hasan et al. 2005), β Cephei (Shibahashi & Aerts 2000) and white dwarfs (Jones et al. 1989). Recently, it has also been proposed that strong magnetic fields exist in the cores of red giants showing depressed dipole modes (Fuller et al. 2015, Cantiello et al. 2016). These fields are invoked to explain the low visibilities of the modes, which are caused by the scattering of gravity waves in the core by the magnetic field. This "magnetic greenhouse effect", as the authors have designated it, leads to the trapping of the waves in that region of the star and prevents the formation of dipole modes with normal amplitudes. This hypothesis is extremely interesting for several reasons, one of them being that it makes an excellent prediction of the depressed mode visibilities. Magnetism in stars is still highly uncharted territory, despite the number of proposed theories regarding the formation and stability of magnetic fields (e.g. Braithwaite & Spruit 2017) and, as such, the confirmation of this conjecture would represent a major step towards understanding this subject.

We organise this work as follows. In section 2 we discuss in more depth the matter of dipole mode depression in red giants, namely the theoretical predictions for the visibility of

depressed modes proposed by Fuller et al. (2015). We then proceed to explain the role of the magnetic field in the mechanism of mode depression. In section 3 we use a new semi-analytical method in the context of red giant seismology to solve the standard wave equation, which we validate by comparing the obtained solutions with the JWKB approximation and the more exact solution obtained using a numerical code. We then analyse the impact of the transmission coefficients computed using the mentioned method in the theoretical visibilities of depressed modes, discussed in section 2. We find that our predictions reproduce the observed results extremely well. Since the most accepted hypothesis for the mechanism responsible for mode depression involves the existence of a magnetic field in the core, in section 4 we investigate for the first time the effect of this field in the frequencies of the oscillation modes. We consider two distinct magnetic fields, validated by numerical simulations, to infer the field strengths that would produce observable frequency splittings and discuss the consequences of these results to the magnetic greenhouse effect hypothesis. We also determine the maximum possible field strength that does not lead to observable magnetic splittings, therefore establishing an upper limit on the value of the field in stars in which magnetic splittings are not observable. Lastly, in section 5 we make a brief summary and present our conclusions.

2. DIPOLE MODE DEPRESSION IN RED GIANTS

An analysis carried out by Mosser et al. (2012) to a group of Kepler red giants revealed that some of these stars exhibit abnormally low dipole mode visibilities. For a mode of angular degree ℓ, its visibility is defined as

$$V_\ell^2 = \frac{\langle A_\ell^2 \rangle}{\langle A_0^2 \rangle} \tag{1}$$

where $\langle A_\ell^2 \rangle$ is the mean value of the square of the amplitude of the mode. An attempt to explain this phenomenon based on rapid rotation of the core was proposed at the time, although it was immediately concluded that it could not be the underlying cause. The measurement of rotational splittings in such stars indicates that their cores spin four to eight times faster than the envelope, a result which is in agreement with what was discovered for other red giants in the same evolutionary stage (Beck et al. 2012). Rapid internal rotation could only produce these effects it the angular velocity was of the same order as the frequencies of the modes showing depression, which is not the case.

A more elaborate explanation for this phenomenon was proposed by Fuller et al. (2015) relying on the existence of strong magnetic fields ($\gtrsim 10^6$ G) in the cores of these stars, which scatter incoming g-waves and prevent them from forming dipole modes with normal amplitudes. This scattering alters the angular structure of the waves and causes their energy to be redistributed over a range of higher mode degrees that, in turn, remain confined to the core. Under the assumption that the waves that are transmitted to the core become trapped and all their energy is completely lost, the authors derived an expression for the ratio of the visibility of a depressed mode and the visibility in the absence of a suppressing mechanism,

$$\left(\frac{V_{\rm sup}}{V_{\rm norm}}\right)^2 = \left(1 + \Delta\nu\tau T^2\right)^{-1} \tag{2}$$

where $\Delta\nu$ is the large frequency separation, τ is the mode lifetime and T is the transmission coefficient through the evanescent region separating the core from the envelope,

$$T = \mathrm{Exp}\left(i\int_{r_1}^{r_2} K\,dr\right) \tag{3}$$

where r_1 and r_2 are the lower and upper boundaries of the evanescent region, respectively, and K is the radial component of the wave-number vector

$$K^2 = \frac{\omega^2}{c^2}\left(1 - \frac{S_\ell^2}{\omega^2}\right)\left(1 - \frac{N^2}{\omega^2}\right). \tag{4}$$

where ω is the angular frequency of the wave. In the previous expression the quantity S_ℓ is the Lamb frequency for modes of angular degree ℓ

$$S_\ell^2 = \frac{\ell(\ell+1)c^2}{r^2}. \tag{5}$$

c is the sound speed, and N is the Brunt–Väisälä or buoyancy frequency,

$$N^2 = g\left(\frac{1}{\gamma}\frac{d\log p}{dr} - \frac{d\log\rho}{dr}\right) \tag{6}$$

where g is the local acceleration of gravity, γ the adiabatic exponent and p and ρ the pressure and density, respectively. Using expression 2, the authors computed the theoretical visibilities of depressed dipole modes with frequencies equal to the frequency of maximum power, $\nu = \nu_{\rm max}$ for a 1.6 $M_\odot$ red giant model, and verified that their predictions were in excellent agreement with the observed visibilities.

The process responsible for mode depression is the creation of strong magnetic tension forces in the core, which arise from the bending of the magnetic field lines by the gravity waves. These forces begin to dominate at a critical value B_c of the magnetic field

$$B_c(r) = \sqrt{\frac{\pi\rho}{2}}\frac{\omega^2 r}{N} \tag{7}$$

and wherever $B > B_c$ magnetic tensions overcome buoyancy, causing transmitted gravity waves to become Alfvén waves. This expression was initially introduced ad hoc but was later proved using the magneto-Boussinesq equations (Lecoanet et al. 2017). The critical field value B_c assumes a minimum value at the H-burning shell, where the Brunt–Väisälä frequency N peaks. Therefore, according to this hypothesis, if a star shows depressed modes a lower limit on the value of the magnetic field in the core can be established. Taking this into account, using data from the Kepler mission, Stello et al. (2016a) studied the visibility of dipole and quadrupole modes in 3600 red giants, with masses under 2.1 $M_\odot$ and frequencies $\nu_{\rm max} \geqslant 50\,\mu$Hz. The authors concluded that the minimum field strength to cause mode depression varies according to the mass and the evolutionary stage of the star in the red giant branch (RGB), and is typically in the range $10^5 - 10^6$ G. They also discovered that red giants with masses under 1.1 $M_\odot$ do not present depressed modes, and above this threshold the number of stars showing mode depression increases with the mass. This fact motivated the idea that these fields are fossil fields, inherited from previous stages of stellar evolution. Stars with masses above this value present a convective core during their MS phase, in which convective motions can generate magnetic fields via dynamo processes. The existence of a dynamo leads to a conversion of

part of the kinetic energy of convective motions into magnetic energy, which results in constant feeding of the field and prevents its dissipation. These fields remain frozen to their mass coordinates, and, subsequently, because of core contraction and assuming magnetic flux conservation, they are amplified in the red giant phase, reaching the mentioned intensities.

3. EFFECT OF WAVE TRANSMISSION IN THE MODE VISIBILITY

3.1. *The standard wave equation*

The 4th-order system describing linear adiabatic stellar oscillations can be reduced to a second-order differential equation by neglecting the perturbation to the gravitational potential (e.g. Gough 1993). This was proposed by Cowling (1941), who showed that this approximation holds quite well except for modes with small values of n and ℓ. The resulting wave equation is

$$\frac{d^2\Psi}{dr^2} + K^2\Psi = 0 \tag{8}$$

where K^2 is given by expression 4 and Ψ is

$$\Psi = \delta p \sqrt{\frac{r^3}{g\rho f}} \tag{9}$$

where δp is the lagrangian perturbation to the pressure and f is the mode discriminant,

$$f = \frac{\omega^2 r}{g} + 2 + \frac{r}{H_g} - \frac{\ell(\ell+1)g}{\omega^2 r} \tag{10}$$

and H_g is the scale height for the gravitational acceleration,

$$H_g = -\frac{dr}{d\ln g}. \tag{11}$$

Solutions to equation 8 are oscillatory wherever $K^2 > 0$, and behave exponentially where $K^2 < 0$. It is straightforward to see that the former behaviour happens wherever $\omega > S_\ell$ and $\omega > N$ or $\omega < S_\ell$ and $\omega < N$ and the latter where $S_\ell < \omega < N$ or $N < \omega < S_\ell$. The radii where $K^2 = 0$ are the turning points and separate the oscillating regions. Red giants in the RGB have two propagating regions, which are separated by four turning points, one at the centre and another at the surface and the remaining two in the interior, between the g-mode and p-mode cavities.

An approximate solution to equation 8 can be derived under the Jeffreys, Wentzel, Kramers and Brillouin (JWKB) approximation. These types of asymptotic solutions have been extensively studied and used in asteroseismology (e.g. Shibahashi 1979; Unno et al. 1989; Gough 1993) and a good summary of the method was carried out by Gough (2007). In an oscillating region, the solution is

$$\Psi = A_1 \left(K^2(r)\right)^{-1/4} \cos\left(\int_{r_1}^{r} \sqrt{K^2(r')}\, dr' - \frac{\pi}{4}\right) \tag{12}$$

where A_1 is a constant and r_1 is the radial coordinate of the lower turning point in the oscillating region. In turn, wherever $K^2 < 0$

$$\Psi = A_2 \left|K^2(r)\right|^{-1/4} \mathrm{Exp}\left(-\int_{r_0}^{r} \left|K^2(r')\right|^{1/2}\, dr'\right) \tag{13}$$

where A_2 is a constant.

3.2. *The phase method*

The solution to equation 8 in the context of the JWKB approximation, presented in the previous section, is not valid for an analysis of the wave function Ψ near the turning points. As can be seen, by expression 12, the amplitude becomes singular at those regions, and an analytical study of the function is not feasible. In view of this problem, to obtain solutions to equation 8 in the form of a product of an amplitude with a sinusoidal term, we used a method developed by H. Prüfer (Prüfer 1926; Chailos 2009). This approach was previously used to study seismic signatures of the acoustic phase in the solar outer layers (Lopes and Gough 2001) and was never applied to the context of wave propagation in red giant stars.

This method consists of transforming a second-order linear differential equation into a couple of two non-linear first-order equations. One of these equations governs the change in the phase with the radial coordinate r, and the other concerns the amplitude. In this approach, the solution can be written as

$$\Psi = A\cos\theta \tag{14}$$

and its derivative as

$$\frac{d\Psi}{dr} = A\sin\theta \tag{15}$$

where $A = A(r)$ is the amplitude and $\theta = \theta(r)$ is the phase. For these relations to hold, these must obey

$$\frac{d\theta}{dr} + \cos^2\theta\left[K^2 - 1\right] + 1 = 0 \tag{16}$$

$$\frac{d\log A}{dr} = \frac{1}{2}\sin(2\theta)\left(1 - K^2\right). \tag{17}$$

The equation that determines the amplitude can also be

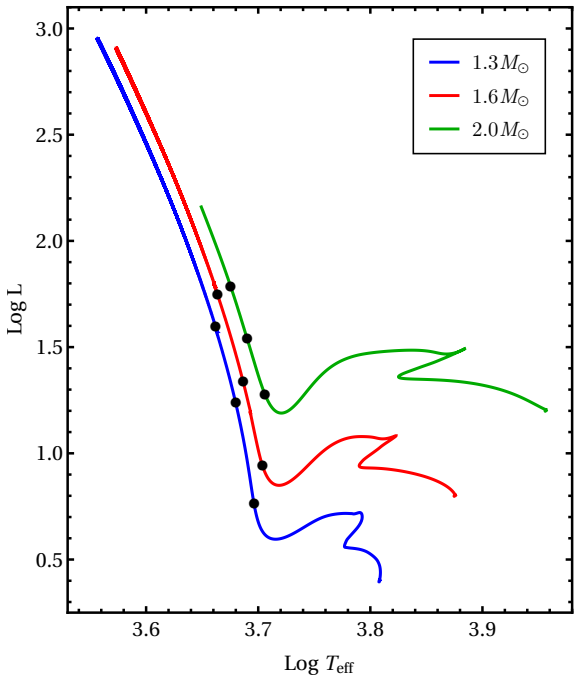

FIG. 1.— Evolutionary tracks for 1.3$M_\odot$, 1.6$M_\odot$ and 2$M_\odot$ stars (blue curve, red curve and green curve, respectively) where the black dots mark the chosen points of the evolution in the RGB to make the comparison between the phase method, GYRE and the JWKB approximation described in text.

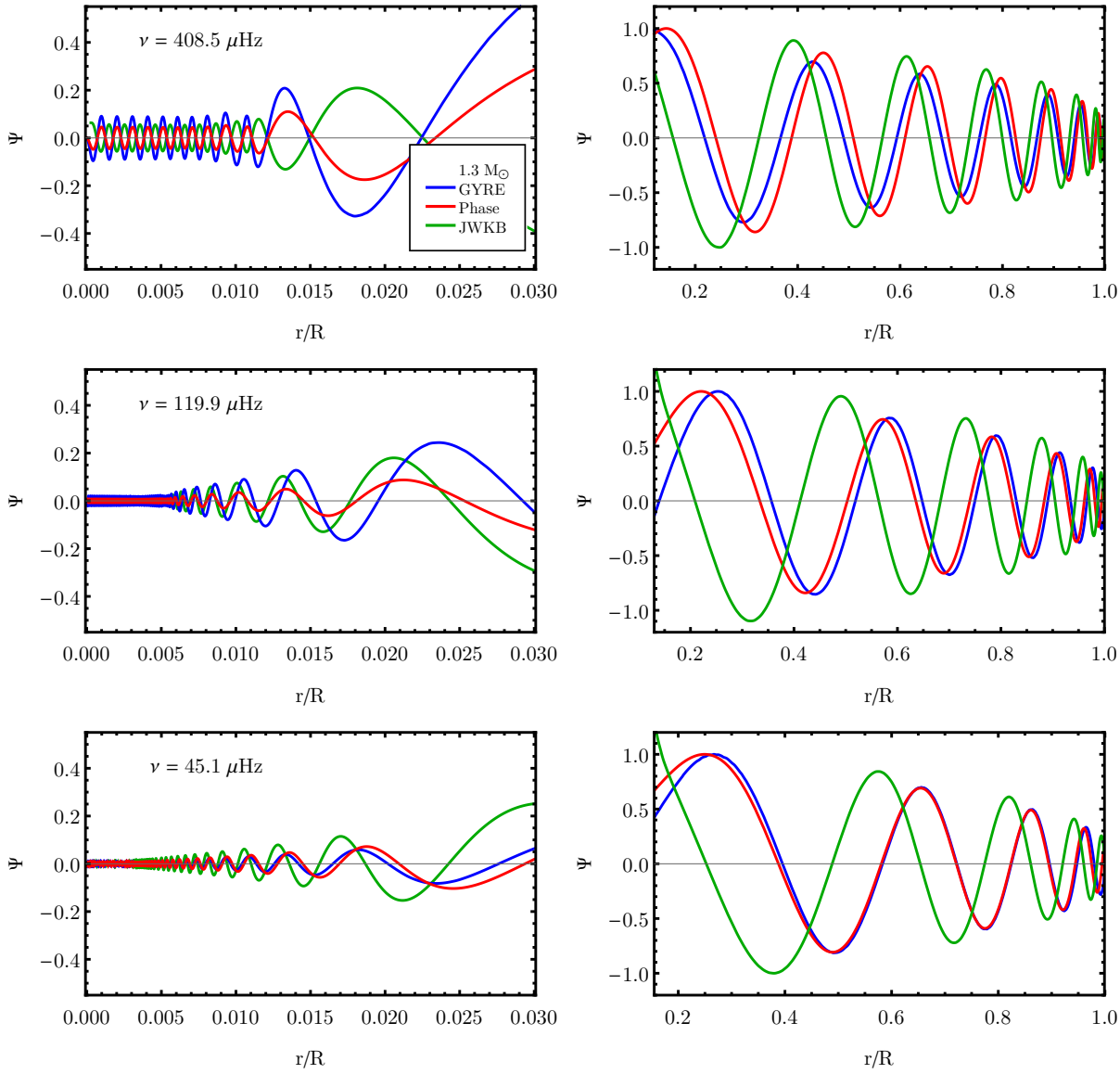

FIG. 2.— Wave function Ψ for dipole waves with frequencies $\nu = \nu_{max}$ obtained with the phase method (red curve) and with GYRE and the JWKB approximation (blue and red curves, respectively) for a $1.3M_\odot$ red giant model at three different evolutionary stages in the RGB. For each of these points we compare the solution inside the g-mode cavity (left plot) and inside the p-mode cavity (right plot).

written

$$A(r) = A_0 \mathrm{Exp}\left[\frac{1}{2}\int_0^r \sin(2\theta)\,(1-K^2)\,dr'\right] \qquad (18)$$

where A_0 is a constant. As can be seen from this expression, the amplitude term is always positive; in fact, the information regarding the overall structure of Ψ, such as its zeroes, is encoded in the phase function θ.

In order to solve the previous equations boundary conditions must be provided. The choice of these is not exactly trivial, as different waves with different frequencies and phases do not need to have the same boundary conditions. In order to generalise them for any wave, we note that Ψ given by expression 9 must satisfy $\Psi \to 0$ as $r \to 0$. In light of this method, this amounts to $\theta \to \pi/2$ as $r \to 0$. No boundary conditions were worked out for the amplitude, because, as can be seen by expression (18), the constant A_0 merely scales the function. One of our purposes with this formalism was to compare the amplitude at different points inside the star, and when taking quotients this term cancels out, so there is no need to define it. From this point further we designate this approach as the 'phase method'.

To build stellar models of red giants we used Modules for Experiments in Stellar Astrophysics (MESA), release 10398 (Paxton and Bildsten 2011, Paxton et al. 2013, 2015, 2018, 2019), using a similar prescription to that used by Fuller et al. (2015). The oscillation frequencies and respective eigenfunctions were computed using GYRE, release 5.1 (Townsend and Teitler 2013), under the Cowling approximation.

In order to test the robustness of the phase method, we compared its solutions with the ones obtained by GYRE and the JWKB approximation. This was done for three different stellar models, with masses $1.3M_\odot$, $1.6M_\odot$ and $2M_\odot$, at three different points in the RGB. These points are represented by the black dots in figure 1, and have been chosen so as to be representative of the validity of the method throughout the whole RGB. We note that we did not verify the method for later ages because these correspond to moments in RGB evol-

ution for which ν_{max} is below 50 μHz, and normally such frequencies are not observable.

The comparison between the three methods for dipole waves with frequencies $\nu = \nu_{max}$ is shown for the $1.3M_\odot$ model in figure 2. The frequency of maximum power was estimated using the scaling relations described by Stello et al. (2013),

$$\nu_{max} = \frac{(M_{star}/M_\odot)}{(R_{star}/R_\odot)^2(T_{eff}/T_\odot)^{1/2}}\nu_{max\odot} \qquad (19)$$

where M is the stellar mass, R is the radius, T_{eff} is the effective temperature and $\nu_{max\odot}$= 3090 μHz. The solution obtained with the phase method is represented by the red curve, and the GYRE and JWKB solutions are represented by the blue and green curves, respectively. All three solutions are normalised to their maximum value in the p-mode cavity. As we can see, the solution obtained with the phase method matches the numerical solution remarkably well, more accurately than the JWKB approximation. This also holds for the other two stellar models, and therefore, with this strong agreement in mind, we expect that for every star with a mass comprehended between $1.3M_\odot$ and $2M_\odot$ the phase method can accurately reproduce the main properties of Ψ in the RGB.

In figure 3 is shown the propagation diagram for the $1.3M_\odot$ model in the RGB, as well as the wave function for a dipole wave with frequency $\nu = \nu_{max}$ as a function of the normalised radial coordinate. The function is normalised to its maximum value in the acoustic cavity, and the vertical dashed grey lines delimit the evanescent region. As can be seen, the wave function is oscillatory in the g-mode and p-mode cavities, blue and red regions, respectively and evanescent in the region separating them.

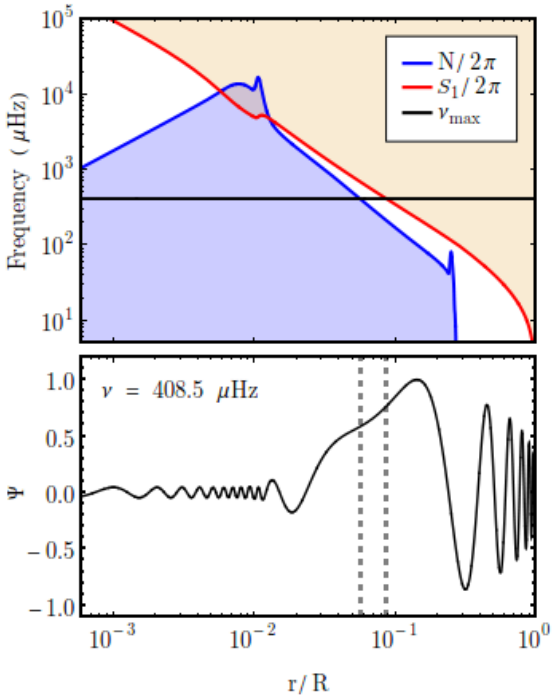

FIG. 3.— Top: propagation diagram for a red giant model with a mass of 1.3 $M_\odot$. The red region is the acoustic cavity for dipole modes and the blue region concerns the gravity mode cavity. The horizontal black line represents ν_{max}, estimated using the scaling relation 19. Bottom: wavefunction Ψ for a dipole wave with frequency ν_{max} = 408.5 μHz, normalised to its maximum in the acoustic cavity, as a function of the fractional radius.

The transmission coefficient in expression 3 is roughly the fractional decrease in wave amplitude across the evanescent region and was derived using an asymptotic analysis by Shibahashi (1979). Our objective in introducing the phase method was to find a way to calculate transmission coefficients more accurately, not resorting to an asymptotic treatment, and to study the subsequent impact on the visibility of depressed modes. With this in mind, we define a transmission coefficient exactly as the fractional decrease in wave amplitude

$$T_P = \mathrm{Exp}\left(-\frac{1}{2}\int_{r_1}^{r_2}\sin(2\theta)\,(1-K^2)\,dr'\right) \qquad (20)$$

where r_1 and r_2 are the lower and upper boundaries of the evanescent region, respectively. As a star ascends the RGB, ν_{max} decreases, and the evanescent region for waves of lower frequencies thickens. Thus, with the exception of one-off cases, the transmission coefficient of waves with frequencies close to ν_{max} should decrease as the star evolves. For T_P determined with expression 3 this is generally true. However, due to the presence of the sinusoidal term in expression 20, T_P may present a slight wiggle when compared for different ages, not being strictly decreasing. In order to smooth out this behaviour, we considered a small interval of frequencies centred around ν_{max} and took the average of the transmission coefficients of these frequencies as the value of T_P for waves with $\nu = \nu_{max}$. The obtained values were, in general, higher than the ones determined with expression 3. In figure 4 we show the resulting visibility band for a 1.6 $M_\odot$ model in the RGB. The blue band was obtained considering T given by expression 3, just like in the work of Fuller et al. (2015), whereas the red band was obtained using the phase method. We considered mode lifetimes in the range $\tau = 5 - 20$ days, the same as the authors and in agreement with the values found by Dupret et al. (2009). The orange dots are the observed dipole mode visibilities of red giants showing mode depression, with frequencies $\nu_{max} > 50$ μHz. This set of data was obtained from an analysis of 3600 red giants performed by Stello et al. 2016a,b. In order to consider just the stars showing mode depression, we filtered this data using the method described in Stello et al. (2016a). As can be seen, our approach reproduces the observed dipole mode visibilities remarkably well, as most of the objects presenting mode depression fall on the red band. In figure 5 we compare the same bands for three different red giant models with masses 1.3 $M_\odot$, 1.6 $M_\odot$ and 2 $M_\odot$, but considering mode lifetimes in the range $\tau = 10 - 30$ days, as in the work of Cantiello et al. (2016). The fact that the bands obtained using the phase method predict lower visibilities for the modes arises from the higher values of T_P in relation to T, as greater wave transmission translates in a greater leakage of wave energy into the core. Since one of the assumptions behind expression 2 is that all the energy that leaks into the g-mode cavity is lost, the amplitudes of the modes will be lower, and consequently so will the visibilities.

4. MAGNETIC FREQUENCY SPLITTINGS BY A MAGNETIC FIELD IN THE CORE

The presence of a magnetic field can modify the oscillation mode pattern by introducing a magnetic frequency splitting (Ledoux & Simon 1957). If the field is weak enough so that it does not substantially change the stellar structure its effect on the frequencies can be studied using a variational approach

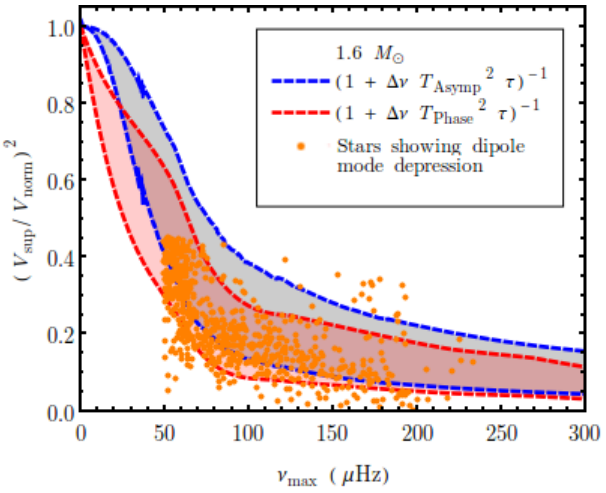

FIG. 4.— Visibility bands for depressed dipole modes as a function of $\nu_{\rm max}$ for a 1.6 $M_\odot$ red giant model in the RGB. The blue band was obtained the same way as Fuller et al. (2015), whereas the red band was obtained using the values of T_P for the transmission coefficient, expression 20. The orange symbols represent the observed visibilities of stars showing dipole mode depression. The experimental data was taken from Stello et al. (2016a,b) and divided by 1.54, as this is the value which normal oscillators are expected to show (Mosser et al. 2012). We used $\tau = 5$ and 20 days (upper and lower curves defining each band, respectively).

(e.g., Unno et al. 1989)

$$\frac{\delta\omega}{\omega} = -\frac{1}{8\pi\omega^2 I}\int [(\nabla\times\mathbf{B}')\times\mathbf{B} + (\nabla\times\mathbf{B})\times\mathbf{B}']\cdot\boldsymbol{\xi}^*\,dV \tag{21}$$

if surface terms are neglected, where I is the mode inertia

$$I = \int \left(\xi_r^2 + \ell(\ell+1)\xi_h^2\right)\rho\, r^2\, dr. \tag{22}$$

and $\mathbf{B}$ is the magnetic field. Assuming a stationary field in the absence of magnetic diffusion, the eulerian perturbation to the magnetic field $\mathbf{B}'$ is

$$\mathbf{B}' = \nabla\times(\boldsymbol{\xi}\times\mathbf{B}) \tag{23}$$

where $\boldsymbol{\xi}$ is, as usual, the displacement vector in the non-magnetic unrotating star,

$$\boldsymbol{\xi} = \left(\xi_r(r)Y_\ell^m, \xi_h(r)\frac{\partial Y_\ell^m}{\partial\theta}, \xi_h(r)\frac{im}{\sin\theta}Y_\ell^m\right)e^{i\omega t}. \tag{24}$$

Using this relation the first term in the numerator of expression 21 can be written in a more simplified manner,

$$-[(\nabla\times\mathbf{B}')\times\mathbf{B}]\cdot\boldsymbol{\xi}^* = |\mathbf{B}'|^2. \tag{25}$$

In this work we use the general expressions for the perturbed field derived by Rashba et al. (2007). We consider two poloidal configurations aligned with the axis of rotation for the magnetic field in the radiative core. The first was initially studied it in the context of neutron stars by Roberts (1981), and takes the form

$$\mathbf{B}_1 = \frac{B_{0,1}}{2}\left(\cos\theta(5-3x^2)\,\mathbf{e}_r + \sin\theta(6x^2-5)\,\mathbf{e}_\theta\right). \tag{26}$$

This field is illustrated on the left side of figure 6, and as can be seen resembles a uniform magnetic field, despite slowly decaying with the radial coordinate. The second field configuration was proposed by Kamchatnov (1982),

$$\mathbf{B}_2 = B_{0,2}\left(\frac{\cos\theta}{(1+y^2)^2}\,\mathbf{e}_r + \sin\theta\frac{(y^2-1)}{(1+y^2)^3}\,\mathbf{e}_\theta\right) \tag{27}$$

where $y = r/Rc$, c being a constant. The magnetic field lines for this configuration are shown on the right of figure 6, and unlike the previous field some of them close inside the core.

The choice of these two fields was motivated by a numerical analysis of their stability in the presence of rotation by Braithwaite (2007). The author verified that both configurations were always unstable, regardless of the angle between the axis of rotation and the axis of the magnetic field, and of the velocity of rotation. This was a confirmation of what was previously known analytically, that purely poloidal or toroidal magnetic fields in radiative regions of stars are always unstable (e.g. Tayler 1973; Wright 1973; Markey and Tayler 1973). Nevertheless, several numerical simulations show that a mixed configuration in which the poloidal and toroidal components of the field have approximately equal strengths can be stable (e.g. Braithwaite and Spruit 2004; Braithwaite and

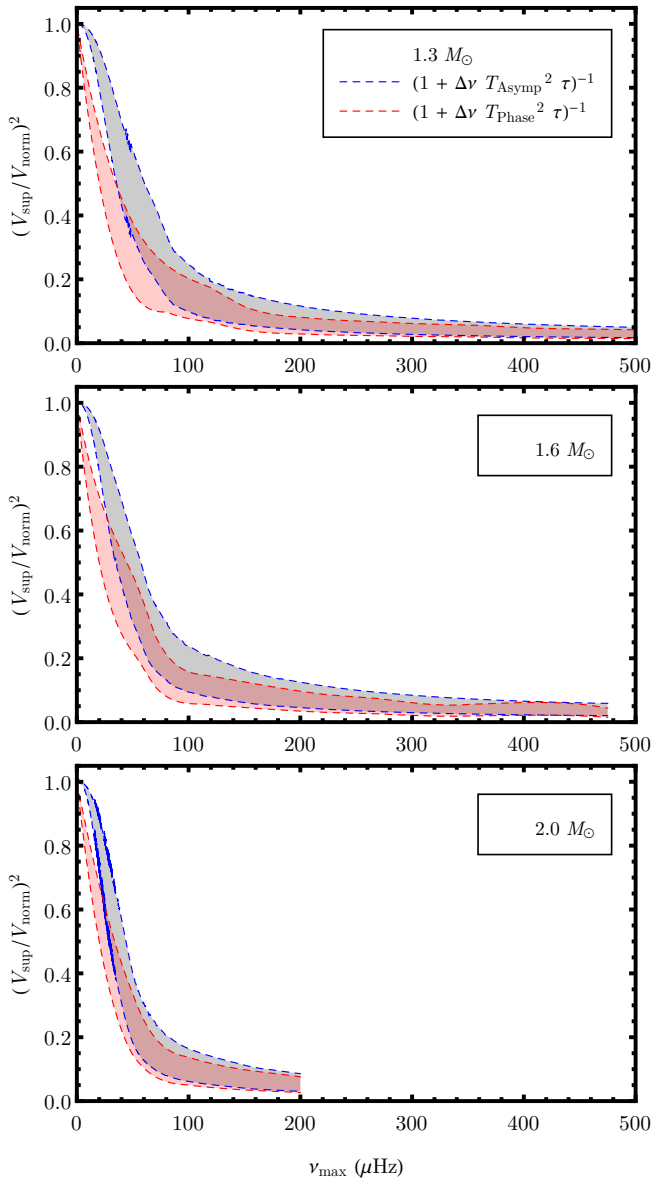

FIG. 5.— The same as in figure 4 but for red giant models with masses 1.3 $M_\odot$, 1.6 $M_\odot$ and 2 $M_\odot$, top, center and bottom plots, respectively. These bands were obtained considering mode lifetimes in the range $\tau = 10 - 30$ days, as in the work of Cantiello et al. (2016).

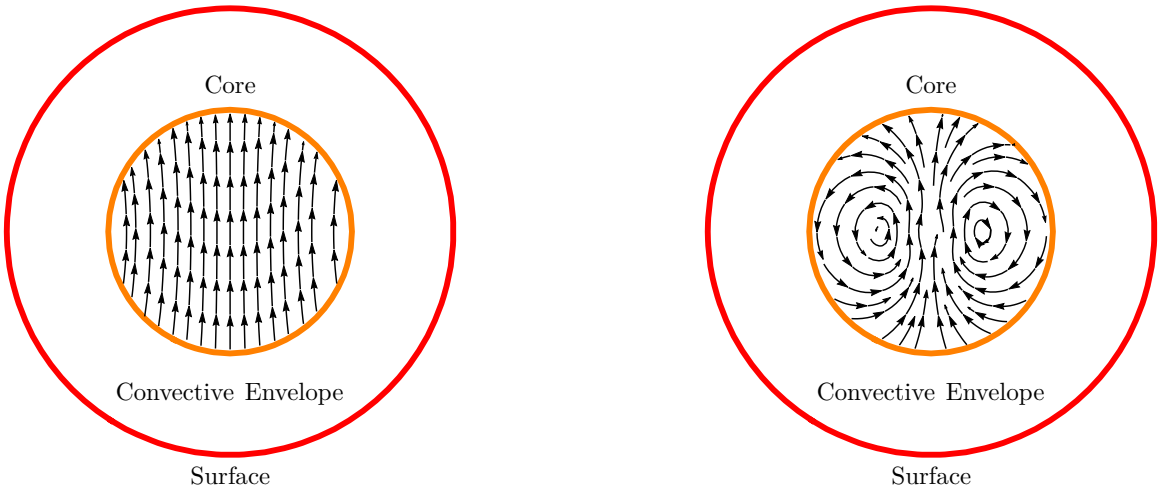

FIG. 6.— Illustration of the magnetic field lines given by expressions 26 (left) and 27 (right). The orange and red curves represent, respectively, the edge of the radiative core and the surface of the star (the figure is not drawn to scale).

Nordlund 2006). Braithwaite's analysis also supports this, revealing that the mentioned fields are capable of evolving into a mixed stable configuration. In particular, the stable state found for the field proposed by Kamchatnov is similar to the ones found in Braithwaite and Nordlund (2006), and therefore these fields may constitute realistic configurations for magnetic fields in radiative zones. As such, their use for the study of magnetic splittings is of interest.

Studies of the character of mixed modes in red giants reveal that a high number of these stars have mixed modes dominated by gravity (e.g Stello et al. 2009). Hence, these g-dominated modes behave almost as pure gravity modes and can be used to probe the physical conditions in the core. In order to study the effect of a magnetic field in the core of a red giant on the frequencies of these modes, we considered the same prescription as in the previous chapter. We evolved a $1.6 M_\odot$ star from the MS to the RGB, stopping at an age of 2.196 Gyr and $\nu_{max} = 123.46\,\mu$Hz. This model is very similar to the one used by Fuller et al. (2015) in their first work proposing the magnetic greenhouse effect. The frequencies of the oscillation modes and the respective eigenfunctions were computed using GYRE in the adiabatic regime, lifting the Cowling approximation, and using the default boundary conditions. The propagation diagram for this model as a function of the normalised stellar mass is shown in figure 7, as well as the horizontal and radial displacement functions ξ_h, ξ_r (blue and red curves of lower plot, respectively) for a dipole mode with $\nu = 123\,\mu$Hz and $n = -98$. As can be seen, the inertia of the modes resides mostly in the core. Since these possess very high radial orders ($|n| \gg 1$) the eigenfunctions are highly oscillatory and the dominant terms in the perturbed magnetic field 23 will be the ones involving the derivatives of ξ_h,

$$|\mathbf{B}'|^2 \simeq \left(\frac{B_0}{R}\right)^2 \left|\frac{2}{x}\frac{d}{dx}(x b_i \xi_h)\right|^2 \left(\left|\cos\theta \frac{\partial Y_m^\ell}{\partial \theta}\right|^2 + \right. \\ \left. + m^2 \left|\frac{\cos\theta}{\sin\theta} Y_m^\ell\right|^2 \right) \tag{28}$$

where $b_1(x) = (5 - 3x^2)/4$ for the field given by expression 26 and $b_2(x) = 1/2(1 + (x/c)^2)^2$ for the field given by 27. We note that the first term inside the integral in expression 21 is quadratic in the derivatives of ξ_h, whereas the second is only linear. Therefore, the latter can be neglected in com-

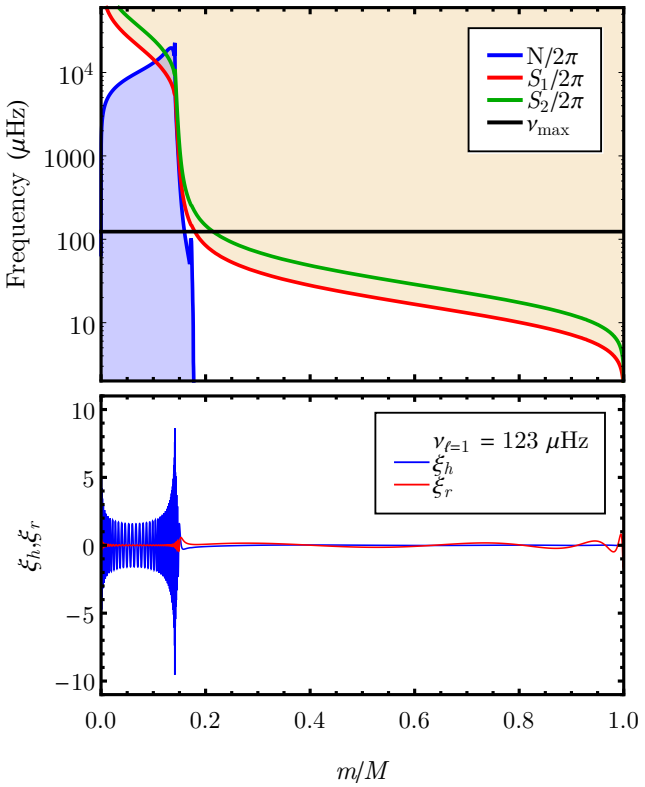

FIG. 7.— Top: propagation diagram for a 1.6 $M_\odot$ red giant model with an estimated $\nu_{max} = 123.46\,\mu$Hz (horizontal black line) as a function of the normalised stellar mass. The blue curve is the Brunt–Väisälä frequency and the red and green curves are the Lamb frequencies for dipole and quadrupole modes, respectively. The region coloured in blue represents the g-mode cavity, and the red region the acoustic cavity for dipole modes. Bottom plot: scaled horizontal and radial displacement eigenfunctions, blue and red curves, respectively, for a dipole mode with $\nu = 123\,\mu$Hz, close to ν_{max}, and radial order $n = -98$.

parison with the former and the expression for the splitting becomes

$$\frac{\delta\omega}{\omega} = \frac{1}{8\pi\omega^2}\left(\frac{B_0}{R}\right)^2 \mathcal{I}\, C_{\ell,m} \tag{29}$$

where

$$\mathcal{I} = \frac{\int \left|\frac{2}{x}\frac{d}{dx}(x b_i \xi_h)\right|^2 x^2 dx}{\int \left(\xi_r^2 + \ell(\ell+1)\xi_h^2\right)\rho\, x^2\, dx} \tag{30}$$

and the coefficients $C_{\ell,m}$ are

$$C_{\ell,m} = \int \left(\left| \cos\theta \frac{\partial Y_m^\ell}{\partial \theta} \right|^2 + m^2 \left| \frac{\cos\theta}{\sin\theta} Y_m^\ell \right|^2 \right) \sin\theta\, d\theta. \tag{31}$$

The insensitivity of these coefficients to the sign of m translates in the magnetic field lifting the degeneracy and producing $\ell + 1$ eigenmodes (Ledoux & Simon 1957).

As we mentioned, a purely poloidal configuration is hydrodynamically unstable and the only known way to achieve stability is if the field has both poloidal and toroidal parts. A toroidal magnetic field aligned with the axis of rotation has only one nonzero component, the azimuthal one, and consequently the dominant term in the respective perturbed field is $|\xi_h|^2$, much smaller than $|\partial\xi_h/\partial_x|^2$ from the poloidal field. Therefore, for g-dominated mixed modes of high radial order, the poloidal field makes most of the contribution to the magnetic splitting and the toroidal part does not have to be considered. We also note that when computing the splittings we are not taking into account the field in the envelope. This is because of two reasons. Firstly, the envelope of a red giant is convective, which means the study of the field in this region must be based on a dynamo theory. The subject of magnetic fields generated by dynamos in the envelopes of these stars is still a largely unexplored and underdeveloped one, because of the complexity of the involved phenomena. The number of studies conducted on this matter is quite scarce, with only a few papers using dynamo theories in the envelopes to explain isotopic abundances in the atmosphere (e.g. Nordhaus et al. 2008). Secondly, most of the inertia of the eigenmodes lies in the core, as can be seen in figure 7, and therefore we don't expect the field in the envelope to play a major contribution.

Since rotational splittings in red giants are typically in the range $10^{-2} - 10^{-1}$ μHz (e.g. Beck et al. 2012; Mosser et al. 2012), we calculated the necessary field strength in the core to produce a splitting of 1 μHz between modes with different values of m, sufficiently distinct from the splittings induced by rotation. Although the mixed mode pattern in red giants is intricate and the task of disentangling rotational splittings and period spacings is highly non-trivial, an automated method for doing so has already been carried out by Mosser et al. (2015) and subsequently put into practice (e.g. Vrard et al. 2016). Therefore, the presence of an extra, magnetic splitting of 1 μHz should be distinguishable with relative ease. The results for the frequencies of three dipole modes are presented in table 1, and for quadrupole modes in table 2. These frequencies were chosen because they are the closest to the estimated frequency of maximum power ν_{max}. For the second field configuration, expression 27, we chose $c = 0.1$. This choice was motivated by the fact that for the stellar model in question the edge of the radiative core is located at $r = 0.1R$. In each of the tables the notation $C_{\ell,m'} - C_{\ell,m}$ denotes the difference $\nu_{\ell m'} - \nu_{\ell m}$ and $B_{core,i}$, with $i = 1, 2$, denotes the field value in the core that would make this difference equal to 1 μHz.

		$C_{1,1} - C_{1,0}$	
$\lvert n\rvert$	ν (μHz)	$B_{core,1}$ (MG)	$B_{core,2}$ (MG)
108	113.66	0.241	0.243
98	123.00	0.269	0.270
88	133.89	0.331	0.332

TABLE 1
VALUE OF THE POLAR MAGNETIC FIELD STRENGTH IN THE CORE THAT WOULD PRODUCE A FREQUENCY SPLITTING OF 1 μHZ IN MIXED DIPOLE ($\ell = 1$) MODES WITH THE INDICATED RADIAL ORDERS AND FREQUENCIES FOR THE TWO FIELD CONFIGURATIONS.

For the dipole mode with the frequency $\nu = 123$ μHz and radial order $|n| = 98$, which is the one closest to ν_{max}, we see that a field strength of 2.7×10^5 G is needed in the core for both fields to produce the mentioned splitting. This order of magnitude is the general trend for the other frequencies as well. Modes with higher values of $|n|$ require lower field strengths to become split, and, as such, from the observational point of view, they are better suited to infer about the intensity of the magnetic field in the core. This makes sense, as these modes have most of their inertia in the core and are more sensitive to the physical conditions of that region.

Cantiello et al. (2016) performed a crude estimate of the magnetic frequency splitting for the model considered in the first work proposing the magnetic greenhouse effect (Fuller et al. 2015). Under the assumption of a purely radial and constant magnetic field with a strength of $B \sim 7 \times 10^5$ G, which is the maximum value that would be allowed without mode depression taking place, the authors found that a splitting of 2 μHz should be observable. This result is remarkably close to ours, although in our analysis we considered validated, realistic field configurations for which the splitting depends on m, and we used the displacement functions computed by GYRE in our calculations.

So far, no red giants exhibiting splittings of magnetic origin have been observed, which seems to suggest that fields of this magnitude do not exist. We can do the opposite reasoning and calculate the maximum field strength that would be allowed in the core without magnetic splittings being detectable. The frequency resolution for the detection of frequency splittings is approximately 11.5 nHz (e.g. Mosser et al. 2012), and, according to our calculations, for a splitting of 11 nHz to occur in dipole and quadrupole modes, tables 3 and 4 respectively, we find that the field has to be of the order of 10^4 G. Therefore, this value constitutes an upper limit to the strength of the magnetic field in the core when magnetic splittings are not observable.

		$C_{1,1} - C_{1,0}$	
$\lvert n\rvert$	ν (μHz)	$B_{core,1}$ (MG)	$B_{core,2}$ (MG)
108	113.66	25.3	25.4
98	123.00	28.1	28.3
88	133.89	34.7	34.8

TABLE 3
VALUE OF THE POLAR MAGNETIC FIELD STRENGTH IN THE CORE THAT WOULD PRODUCE A FREQUENCY SPLITTING OF 1 μHZ IN MIXED DIPOLE ($\ell = 1$) MODES WITH THE INDICATED RADIAL ORDERS AND FREQUENCIES FOR THE TWO FIELD CONFIGURATIONS.

These results have an impact on the magnetic greenhouse

		$C_{2,0} - C_{2,\|1\|}$		$C_{2,0} - C_{2,\|2\|}$		$C_{2,\|1\|} - C_{2,\|2\|}$	
$\|n\|$	ν (μHz)	$B_{core,1}$ (MG)	$B_{core,2}$ (MG)	$B_{core,1}$ (MG)	$B_{core,2}$ (MG)	$B_{core,1}$ (MG)	$B_{core,2}$ (MG)
196	112.69	0.274	0.276	0.137	0.138	0.158	0.159
177	123.39	0.313	0.314	0.156	0.157	0.180	0.181
162	133.24	0.351	0.353	0.175	0.176	0.203	0.204

TABLE 2
VALUE OF THE POLAR MAGNETIC FIELD STRENGTH IN THE CORE THAT WOULD PRODUCE A FREQUENCY SPLITTING OF 1 μHZ IN MIXED QUADROPOLE ($\ell = 2$) MODES WITH THE INDICATED RADIAL ORDERS AND FREQUENCIES FOR THE TWO FIELD CONFIGURATIONS.

effect hypothesis. We recall that this conjecture explains dipole mode depression based on strong magnetic fields in the core of red giants, which scatter transmitted incoming gravity waves and prevent them from interfering and constructing normal dipole modes. This is an extremely interesting and appealing scenario, as it is capable of predicting the visibilities of depressed modes remarkably well and explaining why mode depression only occurs in stars with masses above $1.1M_{\odot}$. In addition, the conversion of gravity waves into Alfvén waves wherever the magnetic field exceeds a critical frequency, proven by Lecoanet et al. (2017), further supports this hypothesis. However, an analysis conducted by Mosser et al. (2017) to a specific group of red giants showing dipole mode depression did not reveal magnetic splittings in stars whose dipole mode amplitudes were low but still measurable. In comparison with the mixed mode pattern of a set of reference stars, which do not present depressed modes, no significant differences in the splittings were observed. If the strong field hypothesis were true, it would be expected that magnetic splittings would also be observable in addition to the reduced amplitudes.

One of the most questionable aspects of the magnetic greenhouse effect hypothesis is that it does not make any prediction about the magnetic field strength when the mode has an amplitude which is abnormally low but still measurable. For the cases of total depression it is possible that the magnetic field has such an influence on gravity waves that these completely suppressed and no magnetic splittings occur, but the intermediate cases are not discussed; in these situations the suppressing mechanism at work cannot cause total energy loss in the core but only a partial energy loss. This situation is the middle ground between no suppression taking place and total suppression. If the agent responsible for this phenomenon is a magnetic field then somewhere between these two scenarios magnetic splittings should be observable. In the case of partial depression, it would be expected that the magnetic field would not be able to suppress gravity waves throughout the core in all its extent but only in a localised region. This means that part of the mode could still survive in the core, instead of living just in the envelope, and lead to measurable magnetic splittings. Therefore, the magnetic greenhouse effect hypothesis remains a plausible one but some of its assumptions should be re-analyzed.

5. SUMMARY AND CONCLUSIONS

In this work we explored some aspects of magnetism in red giant stars, namely the impact on the oscillations of a magnetic field in the core. The issue of magnetic fields in stars is a complicated one, and consequently, despite the growing interest and proposed ideas, it remains a highly open and underdeveloped subject. One of the most effective techniques for testing the proposed theories and reducing the uncertainty around this matter is asteroseismology. Through the observation and analysis of stellar oscillations it is possible to probe the deep interior of stars in a way not possible by direct observation, and hence extract information about the physical conditions in those regions.

The recent discovery of a group of red giant stars in which the dipole modes are absent from the mixed mode pattern or partially depressed led to the idea that this phenomenon is caused by strong magnetic fields in the cores of these stars (Fuller et al. 2015), whose generic properties can be inferred from an analysis of the depression. This scenario is extremely interesting and exciting but still needs more experimental confirmations before being taken as certain.

In the first part of this work we searched for solutions of the standard wave equation using an original method, never used before in this context, consisting on an amplitude and phase decomposition in which we transformed this equation into a couple of first order differential equations. In this semi-analytical approach, one of the equations describes the phase and the other describes the amplitude. By comparison with the solution obtained by the JWKB approximation and the more exact solution obtained using a numerical code, we verified that this approach is capable of reproducing the wave function with great accuracy. Using this important result, we carried out calculations for the transmission coefficients between the envelope and core for different waves and used them in the estimates of the visibility of depressed modes. We found that our results reproduce extremely well the observed ones, evidencing the success of this approach.

In turn, in the second part, we calculated frequency splittings induced by magnetic fields in the cores of red giants. We considered two distinct poloidal axisymmetric magnetic field configurations, validated by numerical simulations, and found that fields of the order of 10^5 G should produce observable splittings of 1 μHz. We also computed the field strength which would result in splittings just below the frequency resolution and found that magnetic fields in the cores of red giants that do not show magnetic splittings should be limited to 10^4 G. These results have important consequences to the magnetic greenhouse effect conjecture, as this hypothesis makes no distinction between the cases of total or partial depression and does not discuss the possibility of the existence of fields which would still be strong but not strong to the point of causing mode depression. Based on our results, if these fields exist they should lead to observable splittings; however, the analysis performed to a group of red giants with partially depressed modes did not reveal any magnetic splittings. If we assume that fields that cause mode depression should also cause magnetic splittings, instead of just suppressing gravity waves, they should be clearly observable. Therefore, the possibility of mode depression being caused by strong magnetic fields is still a plausible one, but further details regarding the mentioned questions need to be addressed.

We are grateful to the authors of MESA and GYRE for hav-

		$C_{2,0} - C_{2,\|1\|}$		$C_{2,0} - C_{2,\|2\|}$		$C_{2,\|1\|} - C_{2,\|2\|}$	
$\|n\|$	ν (μHz)	$B_{core,1}$ (kG)	$B_{core,2}$ (kG)	$B_{core,1}$ (kG)	$B_{core,2}$ (kG)	$B_{core,1}$ (kG)	$B_{core,2}$ (kG)
196	112.69	28.8	28.9	14.4	14.5	16.6	16.7
177	123.39	32.8	32.9	16.4	16.5	18.9	19.0
162	133.24	36.9	37.0	18.4	18.5	21.3	21.4

TABLE 4
VALUE OF THE POLAR MAGNETIC FIELD STRENGTH IN THE CORE THAT WOULD PRODUCE A FREQUENCY SPLITTING OF 1 μHZ IN MIXED QUADROPOLE ($\ell = 2$) MODES WITH THE INDICATED RADIAL ORDERS AND FREQUENCIES FOR THE TWO FIELD CONFIGURATIONS.

ing made their codes publicly available, and to the authors Fuller et al. (2015) for making the MESA inlist used in their work available.

REFERENCES

Aerts, C., Christensen-Dalsgaard, J., Kurtz, D. W. 2010. Asteroseismology. Asteroseismology, Astronomy and Astrophysics Library. ISBN 978-1-4020-5178-4. Springer Science+Business Media B.V., 2010.

Baglin, A., Auvergne, M., Barge, P., et al. 2007. AIP Conference Proceedings, 895, 201

Biront, D., Goossens, M., Cousens, A., Mestel, L. 1982. MNRAS, 201, 3, 619 — 633

Braithwaite, J., Spruit, H.C., 2004. Nature, 431, 819 — 821

Braithwaite, J., Nordlund, Å. 2006. A&A, 450, 3, 1077 — 1095

Braithwaite, J., Spruit, H.C., 2006. A&A, 450, 1097 — 1106

Braithwaite, J., 2007. A&A, 469, 275 — 284

Braithwaite, J., Spruit, H., 2017. RSOS, 4, 2, id.160271

Beck, P.G., Montalban, J., Kallinger, T., et al. 2012. Nature, 481, 55 — 57

Bedding, T.R., Mosser, B., Huber, D., et al. 2011. Nature, 471, 608 — 611

Cantiello, M., Fuller, J., Bildsten, L. 2016. ApJ, 824:14

Chailos, G., 2009. Irish Math. Soc. Bulletin, 63, 11 - 31

Chaplin, W.J., Kjeldsen, H., Christensen-Dalsgaard, J., et al. 2011. Science, 332, 6026, 213 — 216

Chaplin, W.J., Miglio, A., 2013. ARAA, 51, 353 — 392

Cowling, T.J., 1941. MNRAS, 101, 367

Dupret, M.A., Belkacem, K., Samadi, R., 2009. A&A, 506, 1, 55-67

Dziembowski, W., Goode, P. R. 1985. ApJ, 296, L27 — L30

Fuller, J., Cantiello, M., Stello, D., Garcia, R. A., Bildsten, L., 2015. Science, 350, 6259, 423 — 426

Gilliland, R.L., Brown, T.M., Christensen-Dalsgaard, J., et al. 2010. PASP, 122, 131

Goupil, M.J., Mosser, B., Marques, J.P., et al. 2013. A&A, 549, A75

Gough, D. O., Taylor, P.P., 1984. Mem. Soc. Astr. It., 55, 215 — 226

Gough, D. O., Thompson, M.J., 1990. MNRAS, 242, 25 — 55

Gough, D. 1993. in Astrophysical Fluid Dynamics - Les Houches 1987, ed. J.-P. Zahn & J. Zinn-Justin, 399–560

Gough, D. 2007. AN, 328, 3, 273

Hasan, S. S., Zahn, J.-P., Christensen-Dalsgaard, J., 2005. A&A 444, 2, 29 — 32

Prüfer, H., 1926. Math. Ann. (1926) 95: 499

Kamchatnov, A.M., 1982. Zh. Eksp. Teor. Fiz. 82, 117 — 124

Kippenhahn, R., Weigert, A., Weiss, A. 2012. Stellar Structure and Evolution. Stellar Structure and Evolution, Springer-Verlag Berlin Heidelberg, 2012, 2nd ed.

Lagarde, N., Bossini, D., Miglio, A., Vrard, M., Mosser, B., 2016. MNRAS, 457, 21, 59 — 63

Lecoanet, D., Vasil, G. M., Fuller, J., Cantiello, M., Burns, K.J. , 2017. MNRAS, 466, 2, 2181 — 2193

Ledoux P., Simon, R., 1957. Ann. Astrophys. 20, 185

Lopes, I. P., Gough, D., 2001. MNRAS, 322, 3, 473-485

Markey, P., Tayler, R.J., 1973. MNRAS, 163, 1, 77 — 91

Mosser, B., Elsworth, Y., Hekker, S. 2012. A&A 537, A30

Mosser, B., Goupil, M.J., Belkacem, K. 2012. A&A 548, A10

Mosser, B., Vrard, M., Belkacem, K. 2015. A&A 584, id.A50, 10

Mosser, B., Belkacem, K., Pinçon, C. et al. 2017. A&A 598, A62

Nordhaus, J., Busso, M., Wasserburg, G.J., et al. 2008. ApJL, 684, 1, L29

Paxton, B., Bildsten, L., Dotter, et al. 2011. ApJS, 192, 3

Paxton, B., Cantiello, M., Arras, P., et al. 2011. ApJS, 208, 4

Paxton, B., Marchant, P., Schwab, J., et al. 2015. ApJS, 220, 15

Paxton, B., Schwab, J., Bauer, E.B., et al. 2018. The Astrophysical Journal Supplement Series, 234, 2

Paxton, B., Smolec, R., Gautschy, A., et al. 2019. arXiv:1903.01426

Jones, P. W., Pesnell, W. D., Hansen, C. J., Kawaler, S. D. 1989. ApJ, 336, 403-408

Rashbad, T.I., Semikoz, V.B., Turck-Chièze, S., Valle, J.W.F., 2007. MNRAS, 377, 453–458

Roberts, P.H. 1981. Astron. Nach., 302, 65

Roberts, P.H., Soward, A.M., 1983. MNRAS, 377, 4, 1171–1189

Serenelli, J., Johnson, J., Huber, D., et al. 2017. ApJS, 233, 2

Shibahashi, H. 1979. PASJ, 31, 87-104

Shibahashi, H., Aerts, C. 2000. ApJL, 531, L143

Stello, D., Chaplin, W.J., Basu, S., Elsworth, Y., Bedding, T.R. 2009. MNRAS: Letters, 400, Issue 1, L80 — L84

Stello, D., Huber, D., Bedding, T. R., et al. 2013. ApJL, 765, 2

Stello, D. Cantiello, M., Fuller, J., et al. 2016. Nature, 529, 364–367

Stello, D., Cantiello, M., Fuller, J., et al. 2016. PASA, 33, id.e011

Tayler, R.J., 1973. MNRAS, 161, Issue 4, 365–380

Townsend, R.H.D., Teitler, S.A., 2013. MNRAS, 435, Issue 4, 3406–3418

Unno, W., Osaki, Y., Ando, H., Saio, H., Shibahashi, H. 1989. Nonradial oscillations of stars. Nonradial oscillations of stars, San Francisco: W.H. Freeman and Co.,Tokyo: University of Tokyo Press, 1989, 2nd ed.

Vrard, M., Mosser, B., Samadi, R. 2016. A&A, 588, A87

Vrard, M., Mosser, B., Samadi, R. 2016. MNRAS, 162, 4, 339 — 358